Available online at www.sciencedirect.com

ScienceDirect

Journal of Organometallic Chemistry 692 (2007) 4551–4559

Journal of Organometallic Chemistry

www.elsevier.com/locate/jorganchem

Computational study of methane functionalization by a multiply bonded, Ni-bis(phosphine) complex

Thomas R. Cundari *, Aaron W. Pierpont, Sridhar Vaddadi

Department of Chemistry and Center for Advanced Scientific Computing and Modeling (CASCaM), University of North Texas, P.O. Box 305070, Denton, TX 76203-5070, United States

Received 15 March 2007; received in revised form 12 May 2007; accepted 13 May 2007
Available online 2 June 2007

Abstract

A computational chemistry study of nickel-catalyzed group transfer to methane is presented. Two mechanisms were evaluated: a one-step mechanism involving [1+2] insertion of E into the C–H bond of methane, and a two-step $[2_\pi + 2_\sigma]$ mechanism involving addition of the C–H bond of methane across the Ni=E bond to a square planar Ni^{II} intermediate, followed by C–E reductive elimination. Analysis of the energetics for the different mechanistic steps implies a possible competition between the two mechanisms for carbene transfer. For nitrene transfer, the [1+2] pathway is predicted to be the preferred route. Finally, for phosphinidene transfer, the $[2_\pi + 2_\sigma]$ mechanism is calculated to be the preferred mechanism. The two mechanisms studied – [1+2] and $[2_\pi + 2_\sigma]$ – entail exothermic individual reactions, coupled with reasonable enthalpic barriers. Furthermore, regeneration of the catalyst active species by reaction with a group transfer reagent XE is highly exothermic. The calculations thus indicate that (P ∼ P)Ni=E (P ∼ P denotes a chelating bis-phosphine ligand) deserve consideration as plausible starting points in the search for improved hydrocarbon functionalization catalysts.

Keywords: Nickel; Catalysis; Density functional theory; Methane activation; Multiply bonded complexes; Group transfer catalysis

1. Introduction

Aliphatic hydrocarbons are a major component of petroleum feedstocks, and thus their catalytic activation and conversion to functionalized products remains one that is of great scientific and economic interest [1]. Selective carbon–hydrogen bond activation is important as a first mechanistic step in efficient hydrocarbon functionalization, but this must then be followed by carbon–carbon and/or carbon–heterogroup bond formation to give functionalized products. An important component of the desired catalysis is, therefore, to achieve functionalization, which often involves the intermolecular or intramolecular insertion of a heteroatom group (E) into the metal carbon bond (*i.e.*, M–R + E → M–E–R or E–M–R → M–E–R) of an alkyl group (R). Erker's group has beautifully demonstrated such insertion chemistry for early transition metal systems, employing a wide variety of heteroatom groups such as CO, boranes, R–NC, aldehydes, ketones, *etc.* [2]. Once the functionalized alkyl species (M–E–R) is generated, the transfer of a hydrogen from the hydrocarbon substrate regenerates the metal–alkyl intermediate (M–E–R + R–H → M–R + R–E–H) and thus closes the catalytic cycle.

The term "activation" refers to the mechanistic processes by which a metal atom, complex or surface breaks the C–H bond, and σ-bond metathesis, oxidative addition, oxidative hydrogen migration, 1,2-addition, and electrophilic substitution constitute common, nonradical, concerted pathways for carbon–hydrogen bond activation [1]. Later, low-valent complexes typically activate through oxidative addition or a related mechanism that has been termed oxidative hydrogen migration by Goddard and co-workers [3]. Early, high-valent complexes activate C–H bonds via different mechanisms, σ-bond metathesis or 1,2-addition, that do not involve a change in the formal

* Corresponding author. Tel.: +1 940 369 7753; fax: +1 940 565 4318.
E-mail address: tomc@unt.edu (T.R. Cundari).

0022-328X/$ - see front matter © 2007 Elsevier B.V. All rights reserved.
doi:10.1016/j.jorganchem.2007.05.042

oxidation state. In seminal papers, the Wolczanski [4] and Bergman [5] groups demonstrated C–H activation by early transition metal imido complexes (*i.e.*, $L_nM = NR$, where the metal M is typically in a high formal oxidation state and NR is assigned a charge of 2−) through concerted 1,2-addition of the C–H bonds of hydrocarbons (including methane [4]) across the M=N bond. These reactions have been studied extensively using both experimental and computational methods [4,6]. Alas, the resultant Group 4-amido (L_nM–N(H)R) complexes are thermodynamically and kinetically stable, precluding subsequent functionalization and catalyst regeneration pathways.

Until recently, the chemistry of multiply bonded complexes has been the near exclusive domain of complexes involving transition metals from the early and middle portions of the series, most traditionally with metals in high formal oxidation states (d^{0-2}) [7,8]. However, the utilization of new ligand sets, most notably β-diketiminate [9] and bulky, chelating bis-phosphines [10], have yielded new examples of late transition metal multiply bonded complexes. The Warren [11] and Holland [12] groups have demonstrated C–H activation by β-diketiminate nitrene/imido complexes of Ni and Fe, respectively, for activated hydrocarbons such as the bis-allylic C–H bonds of 1,4-cyclohexadiene. The Hillhouse [10] and Warren [11] groups have successfully demonstrated group (nitrene, carbene and phosphinidene) transfer to substrates such as olefins, organic isocyanides, and carbon monoxide. To our knowledge, there have been no experimental reports of a late metal system that both activates aliphatic C–H bonds and then conducts group transfer to yield a complete catalytic cycle for hydrocarbon functionalization, although the report by Vedernikov and Caulton [13] (alkane dehydrogenation coupled to aziridination by a copper catalyst) must be regarded as a very exciting development in this regard.

In the present research, the kinetics and thermodynamics of C–H bond activation and functionalization (insertion of E into a nickel–carbon bond) of methane using (dhpe)Ni=E (E=CH_2, NH, PH) have been investigated, where dhpe = 1,2-bis(dihydrophosphino)ethane), a model of the ligands and complexes studied by Hillhouse and Mindiola [10] for group transfer to olefins. For the present research, the competition between the mode of activation *viz.*, $[2_\pi+2_\sigma]$ and [1+2] addition has been studied, as has the role of the E (carbene, nitrene and phosphinidene) group being transferred to methane.

2. Computational methods

The GAUSSIAN 03 package was used [14]. The B3LYP hybrid density functional was employed [15,16]. For nickel and main group elements the effective core potential (ECP) and valence basis sets of Stephens, Basch and Krauss [17] (CEP-31G) was employed, augmented with a d-polarization function for main group elements (exponent of 0.8 for C and N; 0.55 for P). The -31G basis set was employed for hydrogen. The B3LYP/CEP-31G(d) level of theory has been employed in previous studies and shown to be reliable for the prediction of transition metal geometries and energetics when used in conjunction with a suitable wavefunction or density functional theory technique [18].

All stationary points were singlets and fully geometry optimized using gradient methods without symmetry constraint. Calculated energy Hessians confirmed stationary points as minima (no imaginary frequency) or transition states (one imaginary frequency). Thermochemistry was determined at 1 atm and 298.15 K using unscaled B3LYP/CEP-31G(d) determined frequencies.

3. Results and discussions

The nickel-catalyzed methane functionalization reaction studied here is shown in Eq. (1). For the proposed catalytic cycle, prototypical

$$CH_4 + EX \rightarrow CH_3EH + X \quad (1)$$

group transfer reagents (EX) have been studied. For carbene transfer, the group transfer reagent is diazomethane [10,11], CH_2N_2 and thus $X = N_2$. For nitrene transfer, the model group transfer reagent is hydrazoic acid, HN_3 ($X = N_2$), a simple model of the organic azides that are widely used in the syntheses of late metal nitrene complexes [11,12]. Finally, for phosphinidene transfer, the model group transfer reagent is 7-phosphabicyclo[2.2.1]-heptadiene and thus X = benzene [19].

Two mechanisms of catalytic methane functionalization by (dhpe)Ni have been evaluated [20]: a single-step C–H bond activation and functionalization via a [1+2] transition state; and, a two-step mechanism that proceeds through a $[2_\pi + 2_\sigma]$ transition state. Analysis of the former mechanism is motivated by carbenoid insertion mechanisms such as in the classic Smith–Simmons synthesis [21]. In the [1+2] process, the reaction of the (dhpe)Ni=E complex and methane yields a Ni^0-ligated functionalized product, (dhpe)-Ni(E(H)CH_3), for example, CH_3EH = methylamine in the case of nitrene (NH) transfer, Eq. (2a). The organic product (CH_3EH) is then removed from the nickel center at the expense of an equivalent of group transfer reagent (EX), regenerating the (dhpe)Ni=E active species, and closing the catalytic cycle, Eq. (2b).

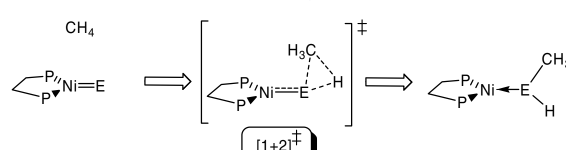

(2a)

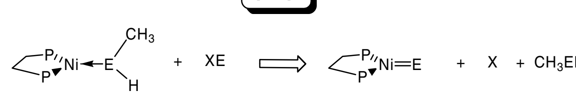

(2b)

In the two-step mechanism, the first step is the reaction of (dhpe)Ni=E with methane to give a (dhpe)Ni^{II}(CH_3)(EH) intermediate via a $[2_\pi + 2_\sigma]$ transition state, Eq. (3a). This is then followed by conversion of the Ni^{II} intermediate through a C–E reductive elimination transition state ($RE^{\neq}$ in Eq. (3b)) to yield (dhpe)Ni^0(E(H)Me).

The two-step mechanism is inspired by the group transfer mechanism for Ni═E complexes proposed by Hillhouse and Mindiola [10] for olefins and studied computationally by our group [22]. As with the [1+2] mechanism, the catalytic cycle for the $[2_\pi + 2_\sigma]$ mechanism is completed by dissociation of the functionalized organic product from the nickel at the expense of EX, Eq. (2b).

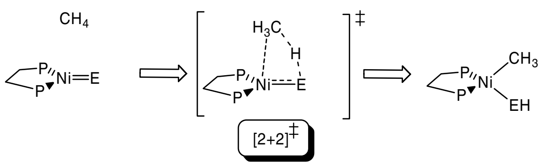

(3a)

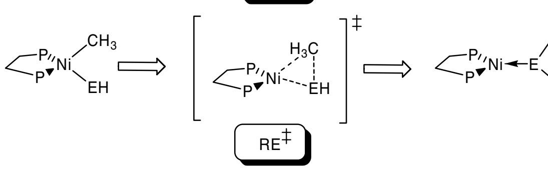

(3b)

3.1. Reactants

Geometry optimization of (dhpe)Ni═E complexes at the B3LYP/SBK(d) level of theory leads to stable, terminally bonded minima for nitrene (E = NH), phosphinidene (E = PH) and carbene (E = CH_2) models as described previously [22]. The minima obtained for carbene, nitrene and phosphinidene complexes have a trigonal planar coordination environment at nickel. Since previous calculations suggested the instability of isovalent (dhpe)Ni═O complexes [22], the present calculations focused on modeling phosphinidene, nitrene and carbene group transfer to methane.

3.2. Transition states

3.2.1. [1+2] Transition state

Calculations were used to first identify a three-centered, triangular [1+2] transition state (TS) ($[1+2]^{\neq}$ in Eq. (2a)) directly connecting the reactants and the functionalized products. The B3LYP/CEP-31G(d) energy Hessian yielded a single imaginary frequency confirming the isolated geometries as first-order saddle points. Intrinsic reaction coordinate (IRC) calculations confirmed that the isolated transition states connect the appropriate reactants ((dhpe)Ni═E + methane) and the metal-bound product ((dhpe)Ni(E(H)CH_3).

Fig. 1 shows two views of a representative [1+2] transition state for nitrene insertion into the C–H bond of methane by (dhpe)Ni = NH. The single imaginary frequency for $[1+2]^{\neq}$ is characterized by substrate activation through the strengthening of E···H as well as C···E bonds and weakening of C···H and Ni···E bonds leading to metal-bound functionalized product, (dhpe)Ni(E(H)CH_3).

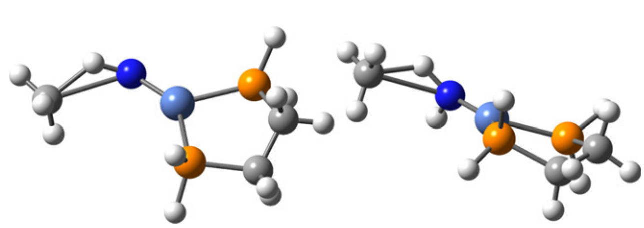

Fig. 1. Two views of the [1+2] transition state for nitrene insertion into the carbon–hydrogen bond of methane.

Comparison of the calculated Ni···E bond lengths in the [1+2] transition state, Table 1, with the NiE bond in the corresponding (dhpe)Ni═E reactant showed an increase of 7% for E = CH_2, 5% for E = NH and 1% for E = PH. A similar comparison of Ni···E in the [1+2] TS vs the corresponding bond in the products showed an increase of 20% for E = CH_2, 13% for NH and 2% for E = PH. The structural comparisons thus suggest a relatively "early" or reactant-like [1+2] transition state for carbene, nitrene and phosphinidene insertion. Full metric data for these and all other calculated stationary points are given in Supplementary material.

3.2.2. $[2_\pi + 2_\sigma]$ Transition state

Calculations at the same level of density functional theory – B3LYP/CEP-31G(d) – were also used to isolate $[2_\pi + 2_\sigma]$ transition states (*i.e.*, $[2+2]^{\neq}$ in Eq. (3a)) for methane C–H bond addition across the Ni═E bond of (dhpe)Ni═E. As before, calculations of the energy Hessian yielded a single imaginary frequency and IRC calculations identified these four-centered transition states as connecting reactants and a (dhpe)Ni^{II}(EH)(CH_3) intermediate, Eq. (3a).

There is an obtuse angle about the hydrogen that is transferred from methyl to E. Hence, from a structural viewpoint these complexes are similar to analogous transition states isolated for methane C–H activation by early metal imido complexes [4,6]. Fig. 2 shows the optimized nitrene $[2_\pi+2_\sigma]$ transition state. The single imaginary frequency is characterized by motion of the hydrogen between the carbon of the methane substrate and the E ligand.

Comparison of the Ni···E bond lengths in the $[2_\pi+2_\sigma]$ transition state, Table 2, with the NiE bond in the corresponding reactants showed an increase of 13% for E = CH_2, 6% for E = NH and 14% for E = PH. A similar comparison of Ni···E in $[2+2]^{\neq}$ vs the corresponding bonds in the products showed an increase of 3% for E = CH_2, 3% for NH and 6% for E = PH. These metric comparisons thus suggest $[2_\pi+2_\sigma]$ transition states for carbene, nitrene and phosphinidene addition that are distinctly later on their

Table 1
Calculated transition state geometries for [1+2] addition of methane to (dhpe)Ni═E[a,b]

E	NiE	EH	EC	CH	EHC
CH_2	1.91	1.20	2.20	1.47	110.2
NH	1.79	1.09	2.40	1.61	123.9
PH	2.12	1.50	2.33	1.47	103.2

[a] Bond lengths in Angstrom units; bond angles in degrees calculated at the B3LYP/CEP-31G(d) level of theory.

[b] Metric data for all stationary points are given in Supplementary material.

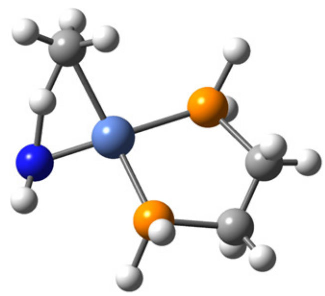

Fig. 2. The $[2_\pi + 2_\sigma]$ transition state for addition of the C–H bond of methane to the nickel-nitrene bond of (dhpe)Ni = NH.

Table 2
Calculated transition state geometries for $[2_\pi + 2_\sigma]$ addition of methane to (dhpe)Ni=E [a,b]

E	NiE	E–H	Ni–C	P_1NiE	P_2NiE
C	1.82	1.56	2.07	95.3	153.5
N	1.80	1.43	2.27	97.9	162.9
P	2.40	1.80	2.09	72.4	162.6

[a] Bond lengths in Angstrom units; bond angles in degrees calculated at the B3LYP/CEP-31G(d) level of theory.
[b] Metric data for all stationary points are given in Supplementary material.

respective potential energy surfaces than the corresponding [1+2] transition states discussed above.

3.3. (dhpe)Ni(CH_3)(EH) intermediate

Distortion of the $[2_\pi + 2_\sigma]$ transition states just discussed along the intrinsic reaction coordinate toward products, followed by geometry optimization yielded square planar (dhpe)Ni(CH_3)(EH) minima (see Fig. 3 for the example of E = NH). Comparison of Ni–E bond measurements of these intermediates with experimental models from the CSD (Cambridge Structural Database) [23] showed considerable proximity between calculated and experimental Ni–E bond lengths (mean ± sample standard deviation; n is the sample size; limited to neutral, four-coordinate Ni(II) complexes with $R < 10\%$): Ni–CH_3 = 1.96 Å (calc.; 1.95 ± 0.03 Å, $n = 39$, expt.), Ni–NH_2 = 1.85 Å (calc.; 1.880 and 1.872 Å for two independent molecules in asymmetric unit of Ni[C_6H_3-2,6-($CH_2P^iPr_2$)$_2$](NH_2)) [24], Ni–PH_2 = 2.25 Å. The nickel–phosphide motif is, to our knowledge, unavailable in the Cambridge Database, although a general search of Ni(four-coordinate)–P(three-coordinate), neutral species, $R < 10\%$, yielded 22 "hits" with a sample mean of 2.20 Å and a sample standard deviation of 0.06 Å [25].

3.4. Reductive elimination transition states

The (dhpe)Ni(CH_3) (E) intermediates just discussed are followed by three-centered reductive elimination transition states ($RE^{\neq}$ in Eq. (3b)), Table 3. Energy Hessian calculations indicated a single imaginary frequency, confirming these geometries as transition states, while the calculated IRCs identified the three-centered transition state as connecting the (dhpe)Ni(CH_3)(EH) intermediate and final products, (dhpe)Ni(E(H)CH_3). The RE transition states entail the weakening of the Ni···E and Ni···C bonds of the Ni^{II} intermediate and lead to formation of the E–C bonds of the functionalized organic product, CH_3EH. Fig. 4 shows a representative reductive elimination transition state for E = NH.

3.5. Reductive elimination products

The reductive elimination transition state leads to a Ni^0 product, (dhpe)Ni(E(H)CH_3), which is an adduct of the functionalized organic product and the formally zero-valent (dhpe)Ni. For E = NH and PH, coordination through a lone pair on the heteroatom is expected and observed (Fig. 5 (top) for E = NH). For the reductive elimination product of E = CH_2 (*i.e.*, ethane) ligation occurs via the σ_{CH} bonds, Fig. 5b.

Table 3
Calculated transition state geometries for reductive elimination of CH_3–E–H from (dhpe)Ni(CH_3)(EH)[a,b]

E	NiE	EC	NiC	CNiE
C	1.97	2.05	1.97	62.8
N	1.82	2.00	2.06	61.8
P	2.14	2.36	2.01	69.2

[a] Bond lengths in Angstrom units; bond angles in degrees calculated at the B3LYP/CEP-31G(d) level of theory.
[b] Metric data for all stationary points are given in Supplementary material.

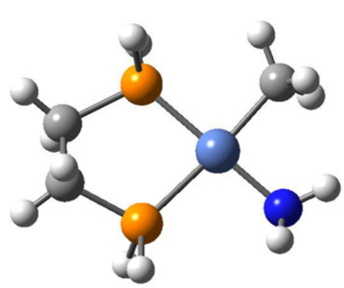

Fig. 3. B3LYP/CEP-31G(d) optimized geometry of the (dhpe)-Ni(CH_3)(NH_2) intermediate.

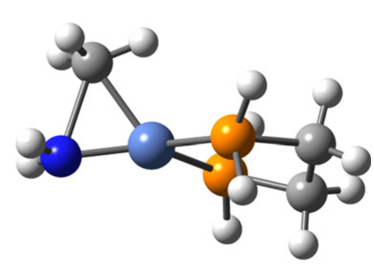

Fig. 4. Reductive elimination transition state for C–N reductive elimination from (dhpe)Ni(CH_3)(NH_2).

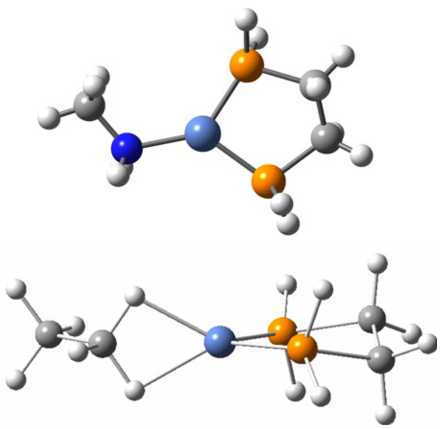

Fig. 5. Reductive elimination products resulting from nitrene transfer (top) and carbene transfer (bottom).

3.6. Study of mechanisms of organic azide decomposition

In order to probe the mechanism for regeneration of the active (dhpe)Ni═E species (Eq. (2b)), model calculations were performed (B3LYP/6-31G(d) as opposed to CEP-31G(d)) for N_2 elimination of from MeN_3 by reaction with (dhpe)Ni. Methyl azide was used in place of hydrazoic acid for the calculations. This chemical alteration was deemed necessary, as it allowed a more appropriate comparison with known organic azide complexes such as those reported by Proulx and Bergman [26], Cummins et al. [27] and Dias and co-workers [28]. The choice of MeN_3 was also motivated by the desire to more accurately model the organic azide reagents used experimentally in the synthesis of late metal nitrenes [11,12]. The calculated thermodynamics for the decomposition of methyl azide leading to nickel-nitrene are given in Fig. 6.

An η^2-methyl azide complex is calculated to be the lowest energy linkage isomer of Ni(dhpe)(N_3Me), Fig. 6. To our knowledge, no crystal structures of Ni(P ~ P) complexes of RN_3 have been reported, although a published conference abstract [29] indicates an η^2 structure, akin to

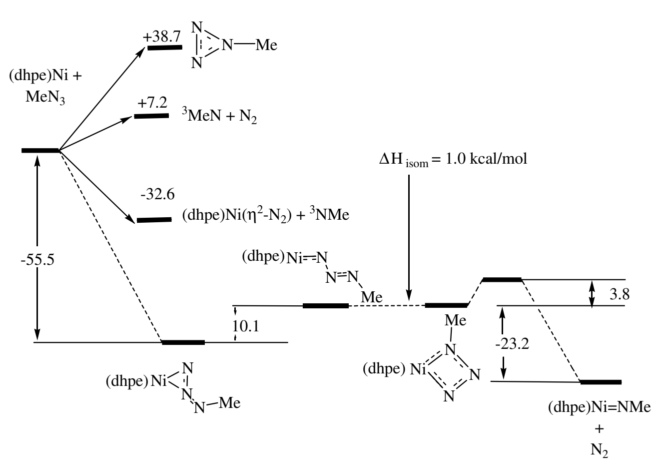

Fig. 6. Calculated reaction diagram for the decomposition of methyl azide. Quoted values are enthalpies (kcal/mol).

the lowest energy linkage isomer found in this research. The most similar experimental model that we are aware of is an η^2-aryldiazo complex reported by Iluc and co-workers: NiN = 1.86 Å; NN = 1.22 Å [30]. Mindiola and Hillhouse reported an η^2-diazoalkane complex as an intermediate in the synthesis of Ni(dtbpe)(═CPh_2), but no crystallographic data was published for the former [10d]. The experimental NiN and NN distances are reasonably commensurate with those calculated for the Ni(dhpe)-(η^2–N_3Me) model complex studied here: NiN = 1.80 Å (two-coordinate nitrogen) and 1.85 Å (three-coordinate nitrogen) and NN = 1.25 Å.

Several pathways for MeN_3 decomposition by Ni(dhpe) were considered. First, we considered metal-independent mechanisms involving initial cyclization of the methyl azide followed by N_2 expulsion or dissociation of N_2 from MeN_3 to form triplet methyl-nitrene. However, the endothermicities of both processes (38.7 kcal/mol and 7.2 kcal/mol, respectively, Fig. 6) ruled these out as candidates for the models under consideration. Two exothermic, metal-dependent pathways were thus considered, the first of which entailed η^2-N_2 adduct formation (with extrusion of triplet NMe) and the second involved the formation of a three-center (dhpe)Ni(η^2-N_3Me) adduct ($\Delta H = -32.6$ kcal/mol and -55.5 kcal/mol, respectively, Fig. 6). The greater stability of the latter induced us to pursue this pathway further. Conversion of (dhpe)Ni(η^2-N_3Me) to the terminally bonded azide (anti conformation) was calculated to be exothermic by 10.1 kcal/mol. Anti/syn isomerization ($\Delta H = +1.0$ kcal/mol) of the terminal azide facilitates formation of a transition state consisting of a four-center NiN_3 unit (3.8 kcal/mol) with subsequent N_2 elimination being very exothermic (-27.0 kcal/mol), Fig. 6.

The scheme summarized in Fig. 6 for MeN_3 decomposition is mirrored experimentally in the synthesis of Re-oxo-imides [31] in which an aryl azide adduct is formed prior to N_2 elimination to afford the corresponding imides. The computed mechanism is also consistent with that proposed for Ta-mediated aryl azide decomposition [26]. Mechanistic studies indicate that Cp_2Ta(Me)–N_3Ph undergoes anti/syn isomerization followed by a similar four-center transition state, which then eliminates N_2 to yield Cp_2Ta(Me) = NPh [32]. However, instead of anti/syn isomerization as the rate determining step, we find conversion of the three-center Ni adduct to the anti adduct ($\Delta H = 10.1$ kcal/mol, Fig. 6) to be the slow step. The model studies indicate that organic azide decomposition by Ni(P ~ P) complexes is a thermodynamically favorable, low barrier process, and thus a suitable candidate for regeneration of the nitrene active species in a catalytic cycle for hydrocarbon functionalization.

4. Thermochemistry

4.1. Reaction enthalpies

The calculated reaction energetics of primary interest are:

(i) The enthalpy of reaction for the formation of the (dhpe)Ni(CH_3)(EH) intermediate (ΔH_{2+2}) arising from the [2+2] addition of a methane C–H bond to (dhpe)Ni=E (Eq. (3a)).
(ii) The enthalpy of reductive elimination (ΔH_{RE}) from the [2+2] intermediate, (dhpe)Ni^{II}(CH_3)(EH), to yield metal-bound product (dhpe)Ni(E(H)CH_3) (Eq. (3b)).
(iii) The overall enthalpy of the reaction ($\Delta H_{rxn} = \Delta H_{2+2} + \Delta H_{RE}$). The latter enthalpy is, of course, the same as the enthalpy for the one-step, [1+2] insertion mechanism, Eq. (2a). Of course, the barriers associated with these processes are also of interest for the insight they may yield on the kinetics of nickel-catalyzed group transfer. The enthalpy to regenerate the (dhpe)Ni=E active species (ΔH_{reg}) from metal-bound product, (dhpe)Ni(E(H)CH_3), and a prototypical group transfer reagent (EX) is also discussed as the reaction models the closing of the catalytic cycle for hydrocarbon functionalization. The calculated reaction enthalpies and enthalpic barriers are organized in Table 4 while the raw data (B3LYP/CEP-31G(d) calculated enthalpies) are given in Table S-2 of the Supplementary material.

For the initial step of the $[2_\pi + 2_\sigma]$ reaction sequence (Eq. (3a)), the calculated enthalpies (ΔH_{2+2}) are exothermic with the phosphinidene reaction being the least exothermic (−9.3 kcal/mol) vs the nitrene (−24.4 kcal/mol) and carbene (−19.2 kcal/mol) reactions, Table 4. The result is similar to that seen in a study of [2+2] addition of the ethylene π-bond to these same (dhpe)Ni=E models [22], and is primarily a reflection of the relatively weak metal-element π-bond strength in these multiply bonded nickel complexes, the stability of the square planar Ni^{II} motif in the intermediate, and the thermodynamic driving force that is realized from the strong Ni–C bond that is formed [33].

For the second step of the [2+2] mechanism (Eq. (3b)), the calculation reaction enthalpies are also exothermic. The reductive elimination process is most exothermic for E = PH, $\Delta H_{RE} = -10.1$ kcal/mol as compared to E = NH ($\Delta H_{RE} = -6.9$ kcal/mol) and E = CH_2 ($\Delta H_{RE} = -6.5$ kcal/mol), Table 4.

As a result of the exothermicity of both the reductive elimination and $[2_\pi + 2_\sigma]$ addition steps, the overall C–H activation *and* functionalization (and, thus of course also direct [1+2] insertion into the C–H bond of methane; $\Delta H_{1+2} = \Delta H_{rxn} = \Delta H_{2+2} + \Delta H_{RE}$) of methane via group transfer is calculated to be highly exothermic for these simple models. Nitrene transfer is the most exothermic ($\Delta H_{rxn} = -31.3$ kcal/mol); phosphinidene transfer is the least exothermic ($\Delta H_{rxn} = -19.4$ kcal/mol) of the reactions studied, while carbene transfer is roughly midway between these two extremes ($\Delta H_{rxn} = -25.7$ kcal/mol).

For a proposed catalytic cycle to be closed, one must regenerate the active species (dhpe)Ni=E and remove the desired organic product from metal. To quantify catalyst regeneration for the systems at hand, we analyzed the thermodynamics of reaction **2b** for prototypical group transfer reagents – hydrazoic acid (HN_3, a simple model of an organic azide), diazomethane (carbene transfer reagent), and 7-phosphabicyclo[2.2.1]-heptadiene (a model of the phosphinidene transfer reagents popularized by Mathey [19]). While the mechanisms of reaction of these group transfer reagents are little studied [26], these reagents, like many that are employed in the synthesis of late transition metal multiply bonded complexes [11,12] attain their kinetic and thermodynamic advantage via the displacement of a weakly bound ligand (CH_3EH) and the production of a very stable inorganic (N_2 for nitrene and carbene transfer) or organic (benzene for phosphinidene transfer) product. It is not surprising, therefore, that these regeneration reactions are highly exothermic (see ΔH_{reg} in Table 4), thus further supporting the feasibility of Ni(P ~ P) systems as possible catalysts for hydrocarbon C–H bond functionalization.

Table 4
Calculated enthalpies for group transfer (kcal/mol)

	E		
	CH_2	NH	PH
ΔH^{a}_{2+2}	−19.2	−24.4	−9.3
ΔH^{b}_{RE}	−6.5	−6.9	−10.1
ΔH^{c}_{rxn}	−25.7	−31.3	−19.4
ΔH^{d}_{reg}	−30.9	−16.7	−19.3
$\Delta H^{\ddagger\,e}_{2+2}$	39.5	29.0	24.7
$\Delta H^{\ddagger\,f}_{RE}$	21.3	26.5	26.8
$\Delta H^{\ddagger\,g}_{1+2}$	31.3	24.8	33.8

[a] Enthalpy of formation of (dhpe)Ni(CH_3)(EH) intermediate from separated reactants, Eq. (3a).
[b] Enthalpy of formation of metal-bound product (dhpe)Ni(E(H)CH_3) from the (dhpe)Ni(CH_3)(EH) intermediate, Eq. (3b).
[c] Total reaction enthalpy, *i.e.*, $\Delta H_{2+2} + \Delta H_{RE}$. This is also the enthalpy for [1+2] insertion, Eq. (2a).
[d] Enthalpy to regenerate the (dhpe)Ni=E active species from a group transfer reagent (XE) and the metal-bound product, (dhpe)-Ni(E(H)(CH_3)), Eq. (2b).
[e] Enthalpic barrier to $[2_\pi + 2_\sigma]$ transition state, Eq. (3a).
[f] Enthalpic barrier to reductive elimination from (dhpe)Ni(CH_3)(EH) intermediate, Eq. (3b).
[g] Enthalpic barrier to [1+2] transition state, Eq. (2a).

4.2. Calculated enthalpic barriers

Given the thermodynamic feasibility of methane functionalization by these simple nickel-catalyst models, we now turn our attention to activation barriers. The calculated enthalpic quantities of interest are summarized in Table 4. For the two-step mechanism, the first step, *i.e.*, $[2_\pi + 2_\sigma]$ carbon–hydrogen bond activation by (dhpe)Ni=E is calculated to possess a higher barrier than reductive elimination for E = CH_2 (39.5 vs 21.3 kcal/mol, respectively). The [2+2] and reductive elimination barriers are more comparable for PH (24.7 vs 26.8 kcal/mol, respectively) and NH (29.0 vs 26.5 kcal/mol, respectively) complexes.

The calculated enthalpic barriers for the single-step mechanism, [1+2] insertion, are comparable to those calculated for the individual steps of the [2+2] mechanism. For the carbene and nitrene complexes the calculated barriers indicate that the preferred pathway to functionalization is the direct [1+2] insertion of E into the C–H bond of methane. For nitrene (carbene) transfer, the calculated barrier to the [1+2] pathway is 4(8) kcal/mol lower than that calculated for the [2+2] barrier, implying that the former will be the preferred route. For phosphinidene transfer, the barrier to [1+2] insertion, 33.8 kcal/mol, is considerably higher (>7 kcal/mol) than that calculated for either step of the two-step mechanism, Table 4, which implies that hydrocarbon functionalization by a nickel–phosphinidene will pass exclusively through a [2+2] pathway with reductive elimination being the rate determining step with a barrier of 26.8 kcal/mol.

Comparing the enthalpic barriers for the preferred mechanisms, the calculations predict greater activity for nickel-catalyzed nitrene ([1+2] barrier = 24.8 kcal/mol) followed by phosphinidene transfer (barrier for the RDS of the [2+2] mechanism is 26.8 kcal/mol), while the analogous nickel-catalyzed carbene transfer (enthalpic barrier for [1+2] insertion is 31.3 kcal/mol).

5. Summary and conclusions

A computational chemistry study of nickel-catalyzed group transfer to methane is presented. Transferred groups studied are nitrene (NH), carbene (CH_2) or phosphinidene (PH). The nickel catalyst studied computationally is a simple model of the bis-phosphine nickel complexes reported by Hillhouse and Mindiola [10] to be stoichiometric group transfer reagents. Two mechanisms were evaluated [20]: (a) a one-step mechanism involving direct [1+2] insertion of E into the C–H bond of methane, and (b) a two-step (or $[2_\pi + 2_\sigma]$ mechanism involving addition of the C–H bond of methane across the Ni=E bond to form a square planar Ni^{II} intermediate, followed by C–E reductive elimination from the intermediate. Several important conclusions have been reached from the present research, the most important of which are summarized here.

(1) Both steps of the $[2_\pi + 2_\sigma]$ mechanism are calculated to be exothermic. Thus, of course, the overall insertion of E into the C–H bond of methane via both mechanisms (*i.e.*, (dhpe)Ni=E + $CH_4 \rightarrow$ (dhpe)Ni(E(H)CH_3)) is therefore exothermic. The calculated exothermicity indicates that from a thermodynamic point of view that these nickel complexes are potent group transfer reagents, as demonstrated experimentally by Hillhouse for CO and olefin substrates [10] and demonstrated here computationally for alkanes, albeit for truncated complex models.

(2) To model the closing of a catalytic cycle, the displacement of organic product (CH_3EH) from the Ni^0-coordination sphere to regenerate the (dhpe)Ni=E active species (*i.e.*, (dhpe)Ni(E(H)CH_3) + XE $\rightarrow$ (dhpe)Ni=E + X + CH_3EH) was studied. Group transfer reagents (XE) modeled include XE = HN_3 (nitrene transfer), CH_2N_2 (carbene transfer), and XE = 7-phosphabicyclo[2.2.1]-heptadiene (phosphinidene transfer). All catalyst regeneration processes were calculated to be energetically very favorable, driven by the formation of a stable X molecule (N_2 for carbene and nitrene transfer; benzene for phosphinidene transfer).

(3) The mechanism for azide decomposition to give nickel-nitrene, a candidate for closure of a catalytic cycle for amination, was studied for E = N–CH_3. A thermodynamic preference was found for the formation of three-center adduct followed by the rate determining formation ($\eta^2 \rightarrow \eta^1$) of an anti (dhpe)Ni–$N_3$Me intermediate that can readily undergo anti/syn isomerization. The syn intermediate promotes cyclization via a four-center transition state ($\Delta H^\ddagger = 3.8$ kcal/mol), which eliminates N_2 to regenerate the (dhpe)-Ni = NMe catalyst in a highly exothermic step. The model studies indicate that nickel-mediated organic azide decomposition is a thermodynamically favorable, low barrier candidate for regeneration of the nitrene active species in a catalytic cycle for hydrocarbon amination.

(4) For the two-step mechanism, the first step, *i.e.*, $[2_\pi + 2_\sigma]$ carbon–hydrogen bond addition to (dhpe)Ni=E is calculated to possess a much higher barrier ($\Delta\Delta H^+ \sim 18$ kcal/mol) than reductive elimination for E = CH_2. The [2+2] and reductive elimination barriers are more comparable ($\Delta\Delta H^+ \sim 2$–3 kcal/mol) with reductive elimination possessing a higher barrier than [2+2] addition for (dhpe)Ni = PH and *vice versa* for (dhpe)Ni = NH.

(5) The calculated enthalpic barriers for a single-step [1+2] mechanism are comparable to those calculated for the individual steps of the [2+2] mechanism. For the carbene and nitrene complexes the barriers suggest that the preferred pathway to functionalization is the direct [1+2] insertion of E into the C–H bond of methane. For phosphinidene transfer, the barrier to [1+2] insertion (33.8 kcal/mol) is considerably higher than calculated for either step of the [2+2] mechanism, which implies that C–H bond functionalization by a nickel–phosphinidene will pass exclusively through a [2+2] pathway with reductive elimination as the rate determining step.

(6) Comparing the enthalpic barriers for the preferred mechanisms, the calculations predict greater activity for nickel-catalyzed nitrene ([1+2] barrier = 24.8 kcal/mol) followed by phosphinidene transfer (barrier for the RDS of the [2+2] mechanism is 26.8 kcal/mol), while the analogous nickel-catalyzed carbene transfer ([1+2] barrier = 31.3 kcal/mol) displays the least activity.

The two mechanisms studied – [1+2] and [2+2] – entail exothermic individual and therefore exothermic overall reactions, coupled with reasonable calculated enthalpic barriers (~25–31 kcal/mol depending on E). Regeneration of the catalyst active species by reaction with a group transfer reagent XE is expected to be facile on the basis of literature precedent, the highly exothermic nature of such reactions, and our preliminary study of the potential energy surface for nickel-mediated decomposition of a model organic azide.

The model complexes evaluated here are very simple mimics, deviating from more plausible experimental systems one might expect in terms of steric factors, for example, the replacement of NDipp with NH (Dipp = 2,6-diisopropylphenyl) or of dtbpe dtbpe = $^{t}Bu_2PCH_2CH_2P^{t}Bu_2$) with dhpe. The electronic and thermodynamic consequences of such chemical elaboration also need to be considered. However, the present calculations indicate that (P ~ P)Ni═E (where P ~ P is a chelating bis-phosphine ligand), and indeed related late transition metal multiply bonded complexes, deserve consideration as plausible starting points in the search for improved catalysts for the functionalization of aliphatic hydrocarbons via group transfer. Such studies of more elaborate models are now underway in our laboratory.

Acknowledgements

The authors acknowledge support of CASCaM by the U.S. Department of Education, and the NSF for their support of the UNT Chemistry Department computational chemistry facility (NSF-CRIF, Grant CHE-0342824). This research is supported by a grant from the This research was supported by a grant from the Offices of Basic Energy Sciences, U.S. Department of Energy (Grant No. DEFG02-03ER15387).

Appendix A. Supplementary data

Supplementary data associated with this article can be found, in the online version, at doi:10.1016/j.jorganchem.2007.05.042.

References

[1] (a) I.J.S. Fairlamb, Ann. Rep. Prog. Chem. B 102 (2006) 50;
(b) L.A. Goj, T.B. Gunnoe, Curr. Org. Chem. 9 (2005) 671;
(c) M. Lersch, M. Tilset, Chem. Rev. 105 (2005) 247;
(d) A.S. Goldman, K.I. Goldberg, Organometallic C–H Bond Activation, ACS, Washington, D.C., 2004;
(e) J.A. Labinger, J.E. Bercaw, Nature 417 (2002) 507;
(f) U. Fekl, K.I. Goldberg, Adv. Inorg. Chem. 54 (2003) 259;
(g) R.H.J. Crabtree, Organomet. Chem. 689 (2004) 4083;
(h) Aaron D. Sadow, T. Don. Tilley, in: 224th ACS National Meeting, Boston, MA, August 18–22, 2002 , INOR-563;
(i) A.D. Sadow, T.D. Tilley, J. Am. Chem. Soc. 127 (2005) 643;
(j) A.S. Goldman, A.H. Roy, Z. Huang, R. Ahuja, W. Schinski, M. Brookhart, Science 312 (2006) 257;
(k) H. Chen, S. Schlecht, T.C. Semple, J.F. Hartwig, Science 287 (2000) 1995;
(l) C.E. Webster, Y. Fan, M.B. Hall, D. Kunz, J.F. Hartwig, J. Am. Chem. Soc. 125 (2003) 858.

[2] (a) U. Blaschke, G. Erker, R. Frohlich, O. Meyer, Eur. J. Inorg. Chem. (1999) 2243;
(b) G. Erker, M. Mena, C. Krueger, R. Noe, Organometallics 10 (1991) 120;
(c) G. Erker, U. Korek, Zeit. Nat. B 44 (1989) 1593;
(d) G. Erker, U. Korek, J.L.J. Petersen, Organomet. Chem. 3550 (1988) 121.

[3] (a) J. Oxgaard, R.A. Periana, W.A. Goddard III, J. Am. Chem. Soc. 126 (2004) 11658;
(b) J. Oxgaard, R.P. Muller, W.A. Goddard, R.A. Periana, J. Am. Chem. Soc. 126 (2004) 352.

[4] (a) C.C. Cummins, S.M. Baxter, P.T. Wolczanski, J. Am. Chem. Soc. 110 (1988) 8731;
(b) C.C. Cummins, C.P. Schaller, G.D. Van Duyne, P.T. Wolczanski, A.W.E. Chan, R. Hoffmann, J. Am. Chem. Soc. 113 (1991) 2985;
(c) C.P. Schaller, P.T. Wolczanski, Inorg. Chem. 32 (1993) 131;
(d) J.L. Bennett, P.T. Wolczanski, J. Am. Chem. Soc. 116 (1994) 2179;
(e) C.P. Schaller, J.B. Bonanno, P.T. Wolczanski, J. Am. Chem. Soc. 116 (1994) 4133;
(f) C.P. Schaller, C.C. Cummins, P.T. Wolczanski, J. Am. Chem. Soc. 118 (1996) 591;
(g) J.L. Bennett, P.T. Wolczanski, J. Am. Chem. Soc. 119 (1997) 10696;
(h) D.F. Schafer II, P.T. Wolczanski, J. Am. Chem. Soc. 120 (1998) 4881.

[5] (a) H.M. Hoyt, F.E. Michael, R.G. Bergman, J. Am. Chem. Soc. 126 (2004) 1018;
(b) P.J. Walsh, F.J. Hollander, R.G. Bergman, J. Am. Chem. Soc. 110 (1988) 8729.

[6] (a) L.M. Slaughter, P.T. Wolczanski, T.R. Klinckman, T.R. Cundari, J. Am. Chem. Soc. 122 (2000) 7953;
(b) T.R. Cundari, T.R. Klinckman, P.T. Wolczanski, J. Am. Chem. Soc. 124 (2002) 1481.

[7] W.A. Nugent, J.M. Mayer, Metal–Ligand Multiple Bonds, Wiley, New York, 1988.

[8] T.R. Cundari, Chem. Rev. 100 (2000) 807.

[9] L. Bourget-Merle, M.F. Lappert, J.R. Severn, Chem. Rev. 102 (2002) 3031.

[10] (a) D.J. Mindiola, G.L. Hillhouse, J. Am. Chem. Soc. 123 (2001) 4623;
(b) R. Melenkivitz, D.J. Mindiola, G.L. Hillhouse, J. Am. Chem. Soc. 124 (2002) 3846;
(c) D.J. Mindiola, G.L. Hillhouse, Chem. Commun. 17 (2002) 1840;
(d) D.J. Mindiola, G.L. Hillhouse, J. Am. Chem. Soc. 124 (2002) 9976;
(e) R. Waterman, G.L. Hillhouse, Organometallics 23 (2003) 5182;
(f) R. Waterman, G.L. Hillhouse, J. Am. Chem. Soc. 125 (2003) 13350;
(g) K.D. Kitiachvili, D.J. Mindiola, G.L. Hillhouse, J. Am. Chem. Soc. 126 (2004) 10554.

[11] E. Kogut, H.L. Wiencko, L. Zhang, D. Cordeau, T.H. Warren, J. Am. Chem. Soc. 127 (2005) 11248.

[12] N.A. Eckert, A. Vaddadi, S. Stoian, C.J. Flaschenriem, T.R. Cundari, E. Munck, P.L. Holland, Angew. Chem., Int. Ed. 45 (2006) 6868.

[13] A.N. Vedernikov, K.G. Caulton, Chem. Commun. 2 (2004) 162.

[14] M.J. Frisch, J.A. Pople, et al., GAUSSIAN 03, Revision C.02, Gaussian, Inc., Wallingford CT, 2004.

[15] (a) A.D. Becke, Phys. Rev. A38 (1998) 3098;
(b) A.D. Becke, J. Chem. Phys. 98 (1993) 1372;
(c) A.D. Becke, J. Chem. Phys. 98 (1993) 5648.

[16] C. Lee, W. Yang, R.G. Parr, Phys. Rev. B37 (1998) 785.

[17] W.J. Stevens, H. Basch, M. Krauss, J. Chem. Phys. 81 (1984) 6026;
W.J. Stevens, H. Basch, M. Krauss, P.G. Jasien, Can. J. Chem. 70 (1992) 612.

[18] (a) Recent examples employing the Steven ECP methodology include the following. J. Vela, S. Vaddadi, S. Kingsley, C.J. Flaschenriem, R.J. Lachicotte, T.R. Cundari, P.L. Holland, Angew. Chem., Int. Ed. 45 (2006) 1607;

(b) J. Vela, S. Vaddadi, T.R. Cundari, J.M. Smith, E.A. Gregory, R.J. Lachicotte, C.J. Flaschenriem, P.L. Holland, Organometallics 23 (2004) 5226;
(c) T.R. Cundari, S. Vaddadi, Inorg. Chim. Acta 357 (2004) 2863.
[19] F. Mathey, Chem. Rev. 90 (1990) 997.
[20] A mechanism involving hydrogen atom abstraction followed by radical rebound to yield metal-bound product was evaluated, but repeated attempts to find a hydrogen atom abstraction transition state yielded the [1+2] insertion transition states discussed herein.
[21] (a) H.E. Simmons, R.D. Smith, J. Am. Chem. Soc. 81 (1959) 4256;
(b) J. Long, Y. Yuan, Y. Shi, J. Am. Chem. Soc. 125 (2003) 13632;
(c) M. Nakamura, A. Hirai, E. Nakamura, J. Am. Chem. Soc. 125 (2003) 2341;
(d) D. Wang, C. Zhao, C.L. Phillips, J. Am. Chem. Soc. 124 (2002) 12903;
(e) A.B. Charette, A. Beauchemin, Org. React. 58 (2001) 1;
(f) W.H. Fang, D.L. Phillips, D. Wang, Y.L. Li, J. Org. Chem. 67 (2002) 154.
[22] T.R. Cundari, S. Vaddadi, J. Mol. Struct. THEOCHEM. 801 (2006) 47.
[23] F.H. Allen, J.E. Davies, J.J. Galloy, O. Johnson, O. Kennard, C.F. Macrae, E.M. Mitchell, J.M. Smith, D.G. Watson, J. Chem. Comput. Sci. (1991) 187.
[24] J. Campora, P. Palma, D. del Rio, M. Mar Conejo, E. Alvarez, Organometallics 23 (2004) 5653.
[25] Cambridge Database, [23] version 5.7, November 2005 with updates through August 2006.
[26] (a) G. Proulx, R.G. Bergman, J. Am. Chem. Soc. 117 (1995) 6382;
(b) G. Proulx, R.G. Bergman, Organometallics 15 (1996) 684.
[27] M.G. Fickes, W.M. Davis, C.C. Cummins, J. Am. Chem. Soc. 117 (1995) 6384.
[28] H.V.R. Dias, S.A. Polach, S.-K. Goh, E.F. Archibong, D.S. Marynick, Inorg. Chem. 39 (2000) 3894.
[29] N.D. Harrold, R. Waterman, G.L. Hillhouse, New group transfer reactions of nickel-carbene and nickel-imido complexes, Abstracts of Papers, 233rd ACS National Meeting, Chicago, IL, March 25–29, 2007, INOR-682.
[30] V.M. Iluc, A.J.M. Miller, G.L. Hillhouse, Chem. Commun. (2005) 5091.
[31] E.A. Ison, J.E. Cessarich, N.E. Travia, O.E. Fanwick, M.M. Abu-Omar, J. Am. Chem. Soc. 129 (2007) 1167.
[32] Proulx and Bergman [26] considered and rejected aryl group transfer and bimolecular decomposition. The former mechanism is calculated to pass through a very high energy (>80 kcal/mol) transition state.
[33] The average NiC bond dissociation enthalpy is estimated as ~45 kcal/mol from the B3LYP/CEP-31G(d) calculated enthalpy of (dhpe)Ni)$(CH_3)_2 \rightarrow$ (dhpe)Ni + C_2H_6 plus the experimental enthalpies (http://webbook.nist.gov/) of formation of ethane and methyl radical.